Available online at www.sciencedirect.com
ScienceDirect
Journal of Sound and Vibration 319 (2009) 320–334
JOURNAL OF SOUND AND VIBRATION
www.elsevier.com/locate/jsvi

Reverberation-ray analysis of moving or distributive loads on a non-uniform elastic bar

J.Q. Jiang, W.Q. Chen*

Department of Civil Engineering, Zhejiang University, Hangzhou 310027, PR China

Received 31 August 2007; received in revised form 22 May 2008; accepted 25 May 2008
Handling Editor: L.G. Tham
Available online 7 July 2008

Abstract

The method of reverberation-ray matrix has been developed and successfully applied to analyze the wave propagation in a multibranched framed structure or in a layered medium. However, the formulation is confined to the case of external concentrated loads applied at the junctions. This paper aims to extend the formulation of reverberation-ray matrix to cases of continuously distributed loads and point moving loads. To this end, a non-uniform bar subjected to these new types of loads is considered for illustration. The difference lies largely in the exact solutions, which include the particular parts due to the loads considered in this paper. The compatibility between displacements in the dual coordinates for a single member is utilized to derive the phase relations. For several types of loadings, numerical results are given and compared with the exact solutions or those obtained by other available method. Exact agreement is observed, thereby validating the present approach. The commonly adopted method that transforms distributed load to equivalent nodal forces is also discussed.

1. Introduction

The method of reverberation-ray matrix (MRRM) has been developed by Pao et al. in a series of publications [1–3] for analyzing planar truss structures subjected to dynamic loads from the viewpoint of wave propagation. The method has been shown to be a potential alternative for dynamic structural analysis, which can predict more accurate dynamic behavior of structures than all available methods [2–4]. The method has also been extended to analyze transient wave propagation in layered media [5,6]. So far, all previous papers on the MRRM [1–6] considered concentrated external loads only. The place where the load acts is a junction or can be modeled artificially as a junction so that within each component (structural member or single layer), there is no external load and only the homogeneous parts (complementary solutions) of the governing equations are employed.

In the MRRM, the most unusual feature is to establish two local coordinates (named as dual local coordinates) for each member, the origins being located at the two ends of the member, respectively. The

*Corresponding author. Tel.: +86 571 87952284; fax: +86 571 87952165.
E-mail addresses: jjiqing@gmail.com (J.Q. Jiang), chenwq@zju.edu.cn (W.Q. Chen).

0022-460X/$ - see front matter © 2008 Elsevier Ltd. All rights reserved.
doi:10.1016/j.jsv.2008.05.031

traveling waves would be expressed exactly by complex eigenfunctions and two teams of unknown coefficients called the local arriving and departing wave amplitudes, respectively, which would be determined by joint conditions and compatibility conditions in each member. From the exact complementary solutions, the reverberation-ray matrix is constructed in the MRRM, which is the product of the global scattering matrix and the phase matrix. The global scattering matrix relates the global arriving wave vector **a** to the departing wave vector **d**. The source vector due to the concentrated loads applied at the junctions (nodes, joints, or interfaces) emerges in this relation. The phase matrix gives another relationship between **a** and **d** according to the phase difference due to the dual local coordinates for each member, and is homogeneous in the case of concentrated loads applied at junctions. For transient analysis, the Fourier or the Laplace transform is usually adopted, and the analysis is first carried out in the transformed domain. The inverse transform should be performed to obtain the time-varying response. The associated integration of specific integrand function, which has many poles, is usually a great obstacle of accurate analysis. In the MRRM, it is supposed to use the Neumann-series expansion technique to avoid the difficulty. Comparison with experimental results [1,2] and other analytical methods [7] indicated that the MRRM is an alternative for dynamic analysis of engineering structures.

Bar is a fundamental type of structure members. Many structures, such as tall buildings and high-rise towers subjected to vertical earthquake motion could be modeled as a bar fixed to a moving base with constant or variable mass and stiffness [8]. In Doyle's monograph [9], a detailed discussion on longitudinal waves in uniform bars is presented and exact solutions of some basic problems can be found. Dynamic response of structures subjected to moving loads has been discussed in Frýba's monograph [10]. Matsuda et al. [11] analyzed the longitudinal impulsive response of non-uniform bars by using two different methods, i.e. the modal analysis and the Laplace transformation.

In this paper, we extend the MRRM to analyze the response of a non-uniform bar subjected to continuously distributed loads as well as point moving loads. The compatibility condition of displacements in dual local coordinates is employed to derive the phase relations. This is different from the previous derivation, which is based on the mechanism of wave propagation. We will show that, instead of an inhomogeneous scattering relation appearing in previous studies [1–6], for the case of continuously distributed loads, the phase relation include inhomogeneous terms. For a uniform fixed–free bar subjected to a harmonic uniform load, the solution is shown to coincide with that obtained by a traditional exact method. It shall be noted that, the bar model is very simple, but it serves as a good example to illustrate our idea of generalizing the current formulation of MRRM to consider loads other than concentrated ones. The formulation for other types of basic structures, such as shafts, Euler–Bernoulli beams, Timoshenko beams, beam–columns and thin-walled structures is similar.

2. Mathematical formulations

First, let us consider the steady-state response of a thin non-uniform bar of length L as shown in Fig. 1(a). The bar is subjected to an external harmonic continuously distributed force $p(x,t)=\overline{p}(x)e^{i\omega t}$ with forcing frequency ω. The force is acting in the direction parallel to the axis of the bar so that the bar is vibrating longitudinally. The mass density ρ, the cross-sectional area A and Young's modulus E can vary arbitrarily along the central line of the bar, i.e. they are all functions of x. It is usually not appropriate to deal with the non-uniform bar directly because the inhomogeneity of the material/geometry makes it very difficult to obtain the solution of the corresponding governing equation, except for some special cases [12]. To overcome the difficulty, we divide equally or non-equally the bar into N sub-bars, each being sufficiently short so that the material/geometric properties can be regarded as constant within sub-bars. Thus, the original non-uniform bar is transformed into N piece-wise uniform sub-bars that are connected one by one as shown in Fig. 1(b).

The governing equation of motion for a uniform bar subject to the harmonic loading is

$$\frac{\partial^2 u(x,t)}{\partial x^2}=\frac{1}{c^2}\frac{\partial^2 u(x,t)}{\partial t^2}-\overline{p}_0(x)e^{i\omega t}, \tag{1}$$

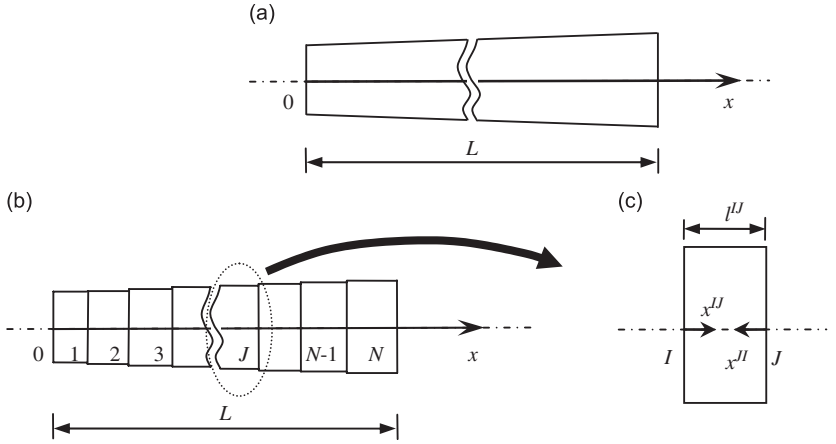

Fig. 1. A non-uniform bar and the piece-wise uniform model.

where $\overline{p}_0 = \overline{p}/EA$, and $c = \sqrt{E/\rho}$ is the longitudinal wave speed. The steady-state solution to this equation is well-known

$$u(x,t) = \left[a\mathrm{e}^{\mathrm{i}kx} + b\mathrm{e}^{-\mathrm{i}kx} - \frac{1}{k}\int_0^x \overline{p}_0(s)\sin[k(x-s)]\,\mathrm{d}s \right]\mathrm{e}^{\mathrm{i}\omega t}$$
$$= \left[A\,\cos(kx) + B\,\sin(kx) - \frac{1}{k}\int_0^x \overline{p}_0(s)\sin[k(x-s)]\,\mathrm{d}s \right]\mathrm{e}^{\mathrm{i}\omega t}, \tag{2}$$

where $k = \omega/c$, a and b are arbitrary complex constants, while A and B are arbitrary real constants. These constants are to be determined by the boundary and continuity conditions.

2.1. Scattering matrix

In MRRM, dual local coordinate systems (with two superscripts) should be introduced. For the sub-bar IJ, as shown in Fig. 1(c), one coordinate system denoted by x^{IJ} originates from the joint I in the positive direction of x, while another coordinate system, x^{JI}, originates from the joint J in the negative direction of x. It is obvious that $k^{IJ} = k^{JI}$, $A^{IJ} = A^{JI}$ and $E^{IJ} = E^{JI}$, etc. At a certain point on the sub-bar, we have $x^{IJ} = l^{IJ} - x^{JI}$ and $\overline{p}_0^{IJ}(x^{IJ}) = -\overline{p}_0^{JI}(l^{IJ} - x^{IJ})$. Changing to the local coordinates so defined, we are able to rewrite the solutions in the two adjacent sub-bars that meet at the joint J as

$$u^{JI} = \left[a^{JI}\mathrm{e}^{+\mathrm{i}k^{IJ}x^{JI}} + d^{JI}\mathrm{e}^{-\mathrm{i}k^{IJ}x^{JI}} - \frac{1}{k^{IJ}}\int_0^{x^{JI}} \overline{p}_0^{JI}(s)\sin[k^{IJ}(x^{JI}-s)]\mathrm{d}s \right]\mathrm{e}^{\mathrm{i}\omega t},$$
$$u^{JK} = \left[a^{JK}\mathrm{e}^{+\mathrm{i}k^{JK}x^{JK}} + d^{JK}\mathrm{e}^{-\mathrm{i}k^{JK}x^{JK}} - \frac{1}{k^{JK}}\int_0^{x^{JK}} \overline{p}_0^{JK}(s)\sin[k^{JK}(x^{JK}-s)]\mathrm{d}s \right]\mathrm{e}^{\mathrm{i}\omega t}, \tag{3}$$

where the term with unknown amplitude d^{JK} represents a wave departing from J and traveling in the positive direction of x^{JK}; while that with a^{JK} represents a wave arriving at J and traveling in the negative direction of x^{JK}. The continuity conditions at J demands

$$u^{JI} + u^{JK} = 0, \quad f^{JI} = f^{JK} \ \text{ at } \ x^{JI} = x^{JK} = 0, \tag{4}$$

where $f^{JI} = E^{JI}A^{JI}\partial u^{JI}/\partial x^{JI}$ is the internal axial force. These conditions lead to a set of equations for the unknown amplitudes

$$\begin{bmatrix} 1 & 1 \\ K^{JI} & -K^{JK} \end{bmatrix}\mathbf{a}^J = \begin{bmatrix} -1 & -1 \\ K^{JI} & -K^{JK} \end{bmatrix}\mathbf{d}^J, \tag{5}$$

where $\mathbf{d}^J=[d^{JI},d^{JK}]^{\mathrm{T}}$ and $\mathbf{a}^J=[a^{JI},a^{JK}]^{\mathrm{T}}$ are local departing and arriving wave vectors, and $K^{JK}=E^{JK}A^{JK}k^{JK}$. Eq. (5) can be rewritten as

$$\mathbf{d}^J=\mathbf{S}^J\mathbf{a}^J \quad (J=1,2,\ldots,N-1). \tag{6}$$

The 2×2 matrix $\mathbf{S}^J$ is called the local scattering matrix at joint J, relating the incident waves to the transmitted and reflected waves. At the two ends (0 and N), the scattering matrices $\mathbf{S}^0$ and $\mathbf{S}^N$ will no longer be 2×2 matrices, instead, both become matrices of single element. For example, for the bar fixed at the left end and free at the right end, we can derive from the boundary conditions

$$\begin{aligned} d^0&=S^0a^0, \quad S^0=-1,\\ d^N&=S^Na^N, \quad S^N=1, \end{aligned} \tag{7}$$

where $d^0=d^{01}$, $d^N=d^{N(N-1)}$, $a^0=a^{01}$, and $a^N=a^{N(N-1)}$.

Now combining $2N$ equations in Eqs. (6) and (7), we can obtain a system of equations for the approximate piece-wisely uniform bar as follows:

$$\mathbf{d}=\mathbf{S}\mathbf{a}, \tag{8}$$

where

$$\begin{aligned} \mathbf{d}&=[d^0,(\mathbf{d}^1)^{\mathrm{T}},(\mathbf{d}^2)^{\mathrm{T}},\ldots,(\mathbf{d}^{N-1})^{\mathrm{T}},d^N]^{\mathrm{T}},\\ \mathbf{a}&=[a^0,(\mathbf{a}^1)^{\mathrm{T}},(\mathbf{a}^2)^{\mathrm{T}},\ldots,(\mathbf{a}^{N-1})^{\mathrm{T}},a^N]^{\mathrm{T}},\\ \mathbf{S}&=\mathrm{diag}[S^0,\mathbf{S}^1,\mathbf{S}^2,\ldots,\mathbf{S}^{N-1},S^N]. \end{aligned} \tag{9}$$

The vector $\mathbf{d}$ is the global departing wave vector, represents waves departing from all joints (points 0, 1, 2,…) leftward and rightward, and the vector $\mathbf{a}$ is the global arriving wave vector, represents waves arriving at all joints rightward and leftward. The $2N\times 2N$ square matrix $\mathbf{S}$ is the global scattering matrix. It can be seen that Eq. (8) is the same as that for the problem without external loads (including distributed and concentrated loads) [1,2].

Notice that both $\mathbf{d}$ and $\mathbf{a}$ are unknown in Eq. (8), which consists of $2N$ equations. Since there are $4N$ unknowns, supplementary equations are necessary.

2.2. Phase matrix and reverberation-ray matrix

We note that, for the same sub-bar, the two solutions in the dual local coordinates should predict the same result. That is, the displacements u^{IJ} and u^{JI} should be compatible to each other, i.e.

$$u^{IJ}(x^{IJ},t)=-u^{JI}(l^{IJ}-x^{IJ},t). \tag{10}$$

Substituting Eq. (3) into Eq. (10) and employing the Euler formula, we obtain

$$a^{IJ}=-\mathrm{e}^{-\mathrm{i}k^{IJ}l^{IJ}}d^{JI}+q^{IJ}, \quad a^{JI}=-\mathrm{e}^{-\mathrm{i}k^{IJ}l^{IJ}}d^{IJ}+q^{JI}, \tag{11}$$

where

$$q^{IJ}=\frac{1}{2\mathrm{i}k^{IJ}}\int_0^{l^{IJ}}\overline{p}_0^{IJ}(s)\mathrm{e}^{-\mathrm{i}k^{IJ}s}\,\mathrm{d}s, \quad q^{JI}=-\frac{\mathrm{e}^{-\mathrm{i}k^{IJ}l^{IJ}}}{2\mathrm{i}k^{IJ}}\int_0^{l^{IJ}}\overline{p}_0^{IJ}(s)\mathrm{e}^{\mathrm{i}k^{IJ}s}\,\mathrm{d}s. \tag{12}$$

Introduce a new local vector, $\overline{\mathbf{d}}^J$, at the joint J, and a new global vector $\overline{\mathbf{d}}$ for the departing waves as

$$\overline{\mathbf{d}}^J=[d^{IJ},d^{KJ}]^{\mathrm{T}}, \quad \overline{\mathbf{d}}=[\overline{d}^0,(\overline{\mathbf{d}}^1)^{\mathrm{T}},(\overline{\mathbf{d}}^2)^{\mathrm{T}},\ldots,(\overline{\mathbf{d}}^{N-1})^{\mathrm{T}},\overline{d}^N]^{\mathrm{T}}, \tag{13}$$

where $\overline{d}^0=d^{10}$ and $\overline{d}^N=d^{(N-1)N}$. The global vectors $\overline{\mathbf{d}}$ and $\mathbf{d}$ contain the same elements but are sequenced in different orders. The two vectors thus can be related through a permutation matrix $\mathbf{U}$ as

$$\overline{\mathbf{d}}=\mathbf{U}\mathbf{d}, \tag{14}$$

where

$$\mathbf{U}=\mathrm{diag}[\mathbf{U}^0,\ldots,\mathbf{U}^0],\quad \mathbf{U}^0=\begin{bmatrix}0 & 1\\ 1 & 0\end{bmatrix}. \tag{15}$$

The inversion of the permutation matrix is just itself.

Thus, Eq. (11) can be rewritten as

$$\mathbf{a}=\mathbf{P}\bar{\mathbf{d}}+\mathbf{q}, \tag{16}$$

where the total phase shift matrix $\mathbf{P}$ $(2N\times 2N)$ is defined by

$$\mathbf{P}=\mathrm{diag}[\mathbf{P}^{01},\mathbf{P}^{12},\ldots,\mathbf{P}^{(N-1)N}],\quad \mathbf{P}^{IJ}=\mathrm{diag}[-\mathrm{e}^{-\mathrm{i}k^{IJ}l^{IJ}},-\mathrm{e}^{-\mathrm{i}k^{IJ}l^{IJ}}] \tag{17}$$

and $\mathbf{q}$ is the source vector due to distributed load,

$$\mathbf{q}=[q^{01},q^{10},q^{12},\ldots,q^{(N-1)N},q^{N(N-1)}]^{\mathrm{T}}. \tag{18}$$

Thus, for the distributed load, the source effect is involved in the phase relations in Eq. (16), while for the concentrated load (applied at the joints only), the source term appears in the scattering relations [1,2]. This is the main difference in the formulations of MRRM between these two types of loadings.

Combining Eqs. (8), (14), and (16), gives

$$(\mathbf{I}-\mathbf{R})\mathbf{d}=\mathbf{s}, \tag{19}$$

where $\mathbf{R}=\mathbf{SPU}$ is named as the reverberation-ray matrix [1,2], and $\mathbf{s}=\mathbf{Sq}$ is the global source vector. After $\mathbf{d}$ is obtained from Eq. (19), the total arriving wave vector is calculated according to

$$\mathbf{a}=\mathbf{PUd}+\mathbf{q}=[\mathbf{PU}(\mathbf{I}-\mathbf{R})^{-1}\mathbf{S}+\mathbf{I}]\mathbf{q}\quad\text{or}\quad \mathbf{a}=\mathbf{S}^{-1}\mathbf{d}. \tag{20}$$

Then substitution of $\mathbf{a}$ and $\mathbf{d}$ into the expressions for internal force and displacement yields the steady-state response of the bar.

If there is no external force, we have $\mathbf{s}=0$. Thus, the frequency equation governing the free vibration of the bar can be obtained by letting the coefficient determinant of Eq. (19) vanish, i.e.

$$\det[\mathbf{I}-\mathbf{R}]=0. \tag{21}$$

2.3. Case study of a uniform bar

Consider a homogenous bar fixed at $x=0$ and free at $x=L$. Starting from the real form solution (with respect to the variable x) presented in Eq. (2), we can easily determine the unknown constants from the boundary conditions as follows:

$$A=0,\quad B=\frac{1}{k\cos(kL)}\int_0^L \overline{p}_0(s)\cos[k(L-s)]\,\mathrm{d}s. \tag{22}$$

Thus, the complete solution is

$$u(x)=\left[\frac{1}{k\cos(kL)}\sin(kx)\int_0^L \overline{p}_0(s)\cos[k(L-s)]\,\mathrm{d}s-\frac{1}{k}\int_0^x \overline{p}_0(s)\sin[k(x-s)]\,\mathrm{d}s\right]\mathrm{e}^{\mathrm{i}\omega t}. \tag{23}$$

If using MRRM, we have

$$\begin{aligned}&\mathbf{d}=[d^{01},d^{10}]^{\mathrm{T}},\quad \mathbf{a}=[a^{01},a^{10}]^{\mathrm{T}},\quad \bar{\mathbf{d}}=[d^{10},d^{01}]^{\mathrm{T}},\\ &\mathbf{S}=\mathrm{diag}[-1,1],\quad \mathbf{U}=\mathbf{U}^0,\quad \mathbf{P}=\mathrm{diag}[-\mathrm{e}^{-\mathrm{i}kL},-\mathrm{e}^{-\mathrm{i}kL}],\\ &\mathbf{q}=\begin{Bmatrix}\frac{1}{2\mathrm{i}k}\int_0^L \overline{p}_0(s)\mathrm{e}^{-\mathrm{i}ks}\,\mathrm{d}s\\ -\frac{\mathrm{e}^{-\mathrm{i}kL}}{2\mathrm{i}k}\int_0^L \overline{p}_0(s)\mathrm{e}^{\mathrm{i}ks}\,\mathrm{d}s\end{Bmatrix}.\end{aligned} \tag{24}$$

Solving for the unknown amplitudes **a** and **d** from Eqs. (19) and (20), we finally obtain the displacement as

$$u(x) = u^{01}(x^{01}) = \left[a^{01}e^{+ikx} + d^{01}e^{-ikx} - \frac{1}{k}\int_0^x \bar{p}_0(s)\sin[k(x-s)]\,ds\right]e^{i\omega t}$$
$$= \frac{e^{i\omega t}}{k\cos(kL)}\sin(kx)\int_0^L \bar{p}_0(s)\cos[k(L-s)]\,ds - \frac{e^{i\omega t}}{k}\int_0^x \bar{p}_0(s)\sin[k(x-s)]\,ds. \quad (25)$$

This is exactly the same as that given by Eq. (23), thus verifying the derivation presented above. If free vibration problem is considered, we can obtain from Eq. (21)

$$k_n = \frac{\omega_n}{c} = \frac{(2n-1)\pi}{2l} \quad (n = 1, 2, 3, \ldots), \quad (26)$$

which also agrees with the well-known result.

It seems rather complicated to apply MRRM to solve this simple problem. However, as has been shown by Pao et al. [1–6], the superiority of this method will be very prominent when dealing with transient dynamic problems, as will be illustrated later.

2.4. Numerical results of a non-uniform bar

Consider a non-uniform bar fixed at $x = 0$ and free at $x = L$, with constant mass density ρ and Young's modulus E. The cross-sectional area varies in an exponential law along the axis, i.e. $A = A_0e^{\alpha x}$ with $\alpha = 1/L$ taken in the calculation. The bar is subjected to a uniformly distributed harmonic force $p(x,t) = p_0e^{i\omega t}$ with $p_0 = EA_0/L$. For the presentation, the quantities are normalized as

$$t = \bar{t}t_0, \quad u = U(\xi,\tau)L, \quad f = F(\xi,\tau)EA_0, \quad \omega = \overline{\omega}/t_0, \quad (27)$$

where $t_0 = L/c$ and $\xi = x/L$.

It is noted that for this particular problem, exact solution could be derived because the governing equation can be transformed into an ordinary differential equation with constant coefficients. The derivation is however omitted here. For the use of MRRM based on the piece-wise uniform model, we divide equally the bar into 20 or 40 sub-bars in the calculation. The normalized axial displacement U and axial force F at $x = 0$ for $\overline{\omega} = 0.3$ are shown in Figs. 2 and 3, respectively.

As shown in Fig. 2, the displacement calculated by MRRM (20 sub-bars) satisfies the boundary condition at the left end perfectly. Comparison of the normalized axial force is also made with the exact solution as shown in Fig. 3. Excellent agreement can be observed. The comparison also indicates that, with the increasing number of sub-bars, the results based on the piece-wise uniform model will approach the exact solution gradually.

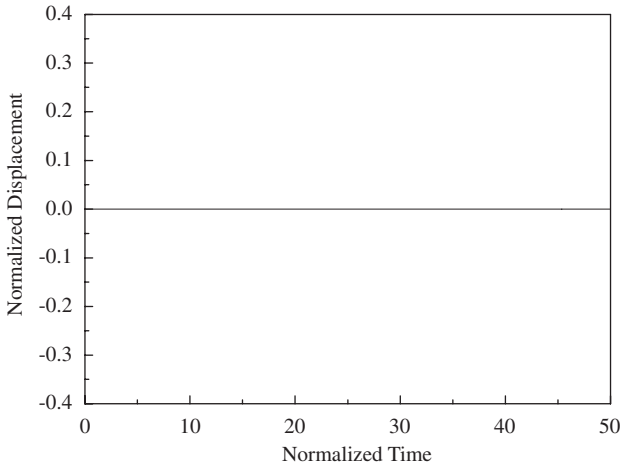

Fig. 2. Normalized axial displacement U at $x = 0$.

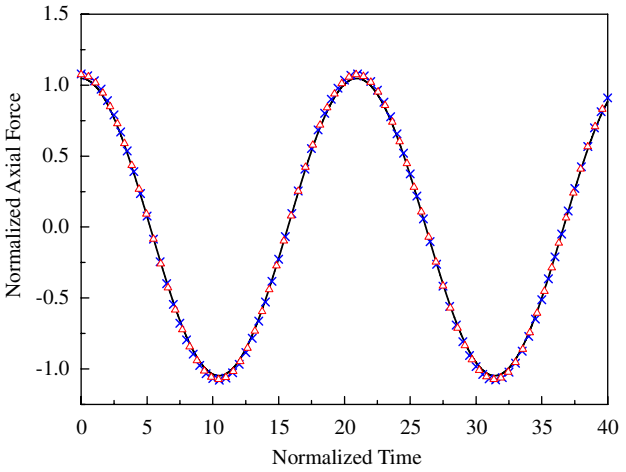

Fig. 3. Normalized axial force F at $x = 0$. — MRRM (20 sub-bars). × MRRM (40 sub-bars). △ Exact.

3. Arbitrary transient response

3.1. General formulation

In the case of an arbitrary time-varying continuously distributed load $p(x,t)$, we shall employ the following Fourier transform:

$$g(t) = \frac{1}{2\pi}\int_{-\infty}^{\infty} \overline{g}(\omega)\mathrm{e}^{\mathrm{i}\omega t}\,\mathrm{d}\omega, \quad \overline{g}(\omega) = \int_{-\infty}^{\infty} g(t)\mathrm{e}^{-\mathrm{i}\omega t}\,\mathrm{d}t. \tag{28}$$

The Fourier transform of the load gives

$$\overline{p}(x,\omega) = \int_{-\infty}^{\infty} p(x,t)\mathrm{e}^{-\mathrm{i}\omega t}\,\mathrm{d}t. \tag{29}$$

It becomes apparent that all derivations in Section 2 keep unaltered, except that the final results thereby obtained are all in the transformed (frequency) domain. Thus, the Fourier inverse transform should be used to obtain the results in the time domain as follows:

$$u(x,t) = \frac{1}{2\pi}\int_{-\infty}^{\infty} \overline{u}(x,\omega)\mathrm{e}^{\mathrm{i}\omega t}\,\mathrm{d}\omega. \tag{30}$$

Since the expression for $\overline{u}$ contains departing and arriving wave amplitudes determined from Eqs. (19) and (20), respectively, the integrand of Eq. (30) has an infinite number of poles, which correspond to the natural frequencies predicted by Eq. (21). This makes it very difficult to obtain accurate numerical results if the integration is carried out directly. To avoid the difficulty, Pao et al. [1,2] suggested to use the following Neumann series:

$$(\mathbf{I}-\mathbf{R})^{-1} = \mathbf{I} + \mathbf{R} + \mathbf{R}^2 + \cdots + \mathbf{R}^N + \cdots, \tag{31}$$

when calculating the departing wave vector in the frequency domain. This technique removes the singularities due to the poles in the integration (and hence greatly improve the numerical accuracy), and also embodies the wave propagation procedure in each member of the structure. A detailed discussion on the Neumann-series expansion and the selection of various parameters in the integration can be found in Pao et al. [1–3,7].

It is emphasized that, if the spectral element method [13], which is also based on the exact solutions is employed, it is impossible to employ the Neumann series in Eq. (31) to remove the poles in the integrand. Although small damping could be introduced artificially to avoid the singularities, its value largely depends on the problem under consideration, and hence the experience of the researcher becomes crucial to obtaining accurate results [13].

3.2. Numerical results

Consider again a non-uniform bar with fixed–free boundaries, subjected to the following time-stepped uniformly distributed force:

$$p(x,t)=\begin{cases} EA_0/(10,000L), & 0\leqslant t\leqslant 6t_0. \\ 0, & t>6t_0. \end{cases} \tag{32}$$

The cross-sectional area varies according to $A=A_0e^{-x/L}$, and the bar is divided into 20 sub-bars in the calculation. The normalized axial force at $\xi=0.25$ and $0.5L$ are given in Fig. 4. It can be shown that after the remove of the external load, the axial force still varies with the time since no damping has been included in the analysis. Actually, the response will tend to be steady and can be viewed as the response of the bar due to an appropriate initial disturbance.

The results calculated by MRRM are also compared with those by the commercial software ANSYS as indicated in Fig. 5. It is shown that the two results coincide with each other very well. One of the advantages of MRRM is that the total number of sub-bars required in the calculation could be much less than that normally used in the conventional finite element method (FEM) to achieve the same numerical accuracy. In this example, the non-uniform bar is approximated by 160 finite elements and the time step is taken to be 5×10^{-6} s. Consequently, the numerical efficiency of the FEM is significantly lower than MRRM.

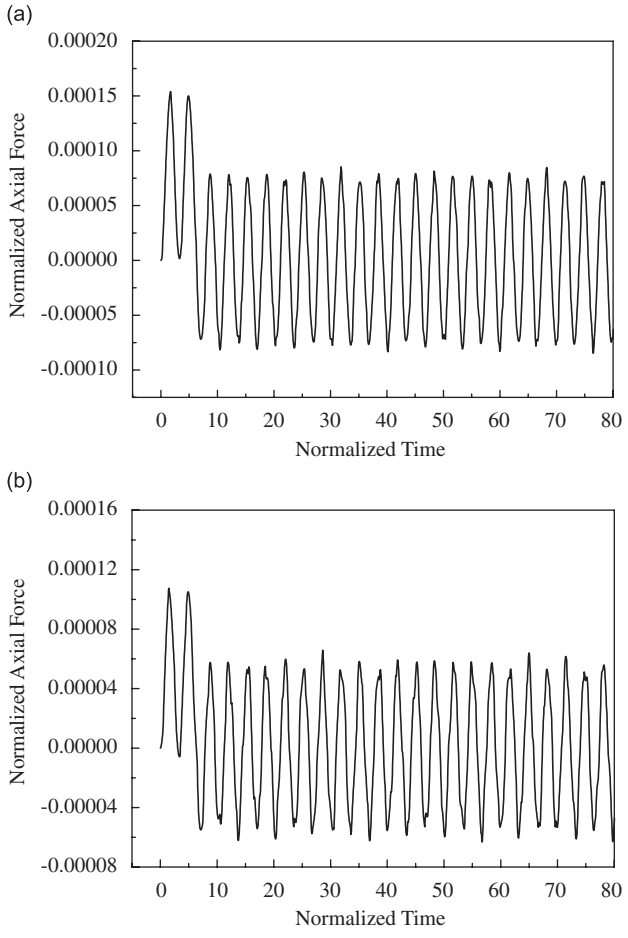

Fig. 4. Normalized axial force F at (a) $\xi=0.25$, and (b) $\xi=0.5$.

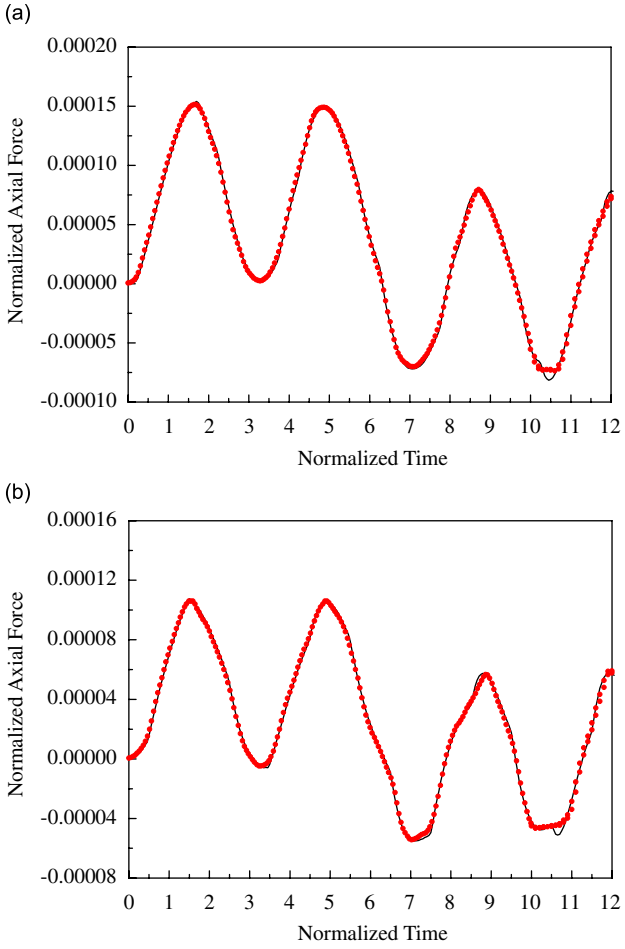

Fig. 5. Comparison of normalized axial force F at (a) $\xi = 0.25$, and (b) $\xi = 0.5$. — MRRM. ····· ANSYS.

In order to illustrate the application of the present method, we further consider a linearly varying external force as follows:

$$p(x,t) = \begin{cases} \dfrac{EA_0}{L^2}x, & 0 \leqslant t \leqslant 6t_0, \\ 0, & t > 6t_0. \end{cases} \tag{33}$$

For the same non-uniform bar considered above, the axial strain at the mid-span is shown in Fig. 6, which again agrees well with the result obtained by Ansys.

As the third example, we consider a fixed–fixed uniform bar loaded both by a distributed force $p(x,t) = 10EAx(L-x)/L^3$ within $0 \leqslant x \leqslant 0.3L$ and a concentrated force $f_e = EA$ at $x = 0.8L$. The periods of duration of the two forces are assumed to be $8t_0$ and $10t_0$, respectively. To solve this problem, we first divide the bar into three segments (sub-bars 01, 12, and 23) as shown in Fig. 7(a). Since there is no distributive load applied onto sub-bars 12 and 23, the particular solution in the expression of displacement vanishes. The continuity conditions at joint 2, where the concentrated force f_e is applied, should be revised as

$$EA\frac{\partial u^{23}}{\partial x^{23}} + f_e = EA\frac{\partial u^{21}}{\partial x^{21}} \quad \text{at} \quad x^{21} = x^{23} = 0. \tag{34}$$

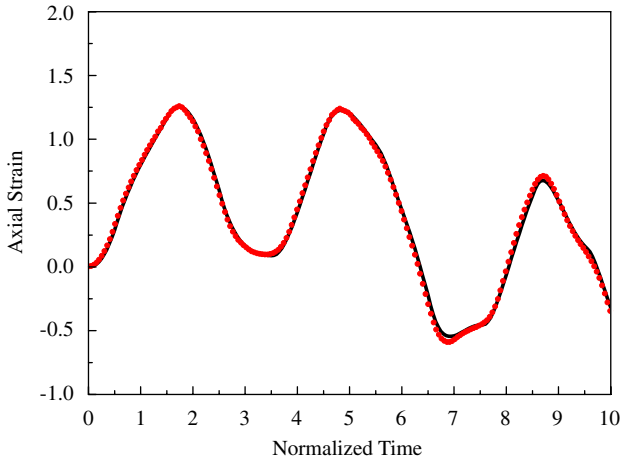

Fig. 6. Axial strain at $\xi = 0.5$. — MRRM. ····· ANSYS.

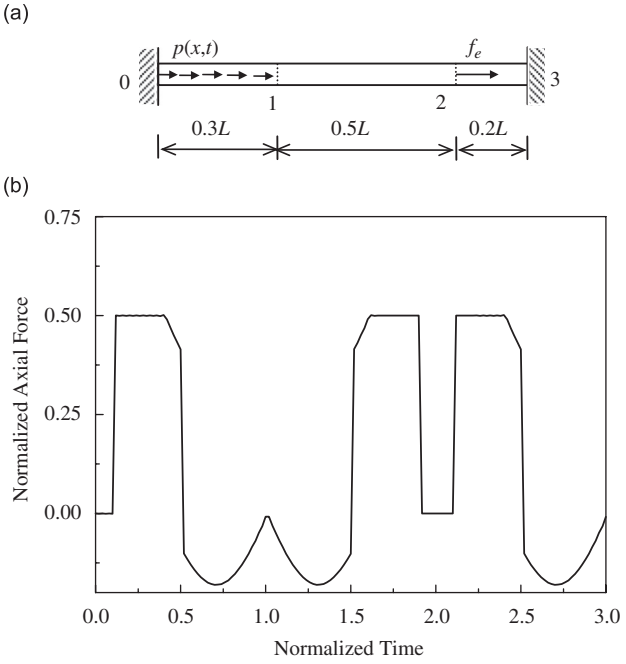

Fig. 7. (a) Sketch of a fixed–fixed uniform bar. (b) Normalized axial force at $\xi = 0.7$.

The scattering relation such obtained contains a source vector and has the form of $\mathbf{d} = \mathbf{Sa} + \mathbf{s}_1$. The other derivations and the form of Eq. (19) keeps unaltered except $\mathbf{s} = \mathbf{Sq} + \mathbf{s}_1$.

The normalized axial force $F(\xi,\tau) = f/EA_0$ at $\xi = 0.7$ is calculated and shown in Fig. 7(b). For $0 \leqslant \tau < 0.1$, there is entirely no dynamic response at $\xi = 0.7$. At the instant of $\tau = 0.1$, the wave generated by the concentrated external force f_e arrives at that point, and a stepped response can be observed with the amplitude being one half of the force f_e. Later at $\tau = 0.4$, the wave excited by the distributed load also arrives, resulting in an obvious change in the waveform as we can see from Fig. 7(b). Actually, from the change of the waveform, the wave propagating along the rod and scattering at joints can be clearly identified. Thus, the present method can give an accurate prediction of transient response of structures especially at the early time.

3.3. Discussion on the method of equivalent nodal forces

In the FEM, the distributed forces are usually replaced by equivalent nodal forces by using the principle of equilibrium of virtual work. For a one-dimensional bar element, this gives

$$\begin{Bmatrix} F(0) \\ F(l) \end{Bmatrix} = \int_0^l \mathbf{N}^{\mathrm{T}} p(x,t)\,\mathrm{d}t, \tag{35}$$

where $\mathbf{N} = [1-x/l \; x/l]$ is the shape function, and $F(0)$ and $F(l)$ are the equivalent nodal forces for an arbitrary distributed load $p(x, t)$ applied over the element $0 \leqslant x \leqslant l$. Under such an approximation, the problem with distributive load is transformed to the one with concentrated forces only, and the traditional MRRM [1,2] can be employed directly.

Now we consider a fixed–free uniform bar subject to a constant distributed load $p(x, t) = EA/L$ $(0 \leqslant t \leqslant 6t_0)$. The responses obtained based on the present formulations for distributed load and those by the traditional MRRM using the concept of equivalent nodal forces are compared in Fig. 8. As we can see, the traditional results get closer to the present ones with the increasing number of elements. The convergence of axial force is worse than the displacement, and hence a much finer mesh is needed to obtain accurate transient force response, which also means a reduction in the numerical efficiency.

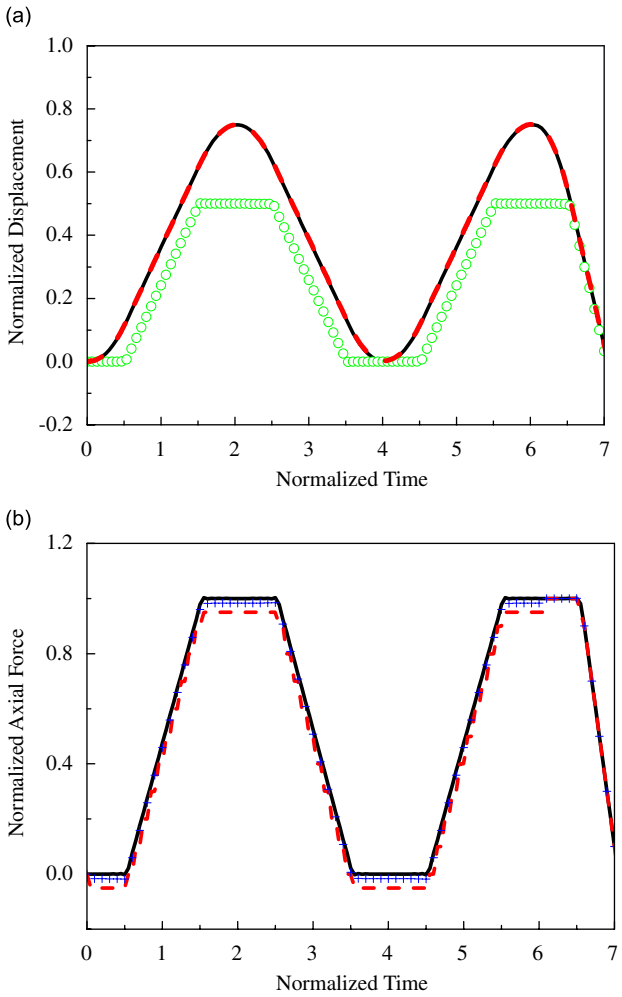

Fig. 8. (a) Normalized displacement at $\xi = 0.5$. (b) Normalized axial force at $\xi = 0.5$. — distributed load (1 element). ○ Equivalent nodal force (1 element). ---- Equivalent nodal force (10 elements). + Equivalent nodal force (30 elements).

4. Case of a point moving load

4.1. A uniform rod subjected to a point moving load

First, we consider a uniform bar subject to a point moving load $p(x,t)=p_\delta\delta(x-a_0t)$. In this case, by applying the Fourier transform to the governing equation, we obtain

$$\frac{\mathrm{d}^2\overline{u}(x,\omega)}{\mathrm{d}x^2}+k^2\overline{u}(x,\omega)=-\frac{p_e}{a_0}\mathrm{e}^{-\mathrm{i}\omega x/a_0}, \tag{36}$$

where $p_e=p_\delta/(EA)$. The solution to this equation can be written as

$$\overline{u}(x,\omega)=a\mathrm{e}^{\mathrm{i}kx}+d\mathrm{e}^{-\mathrm{i}kx}-p_1\mathrm{e}^{-\mathrm{i}k_1x}, \tag{37}$$

where $k_1=\omega/a_0$ and $p_1=p_e/[a_0(k^2-k_1^2)]$. Thus, in the two local coordinates (0-1 and 1-0) for the uniform rod, we have

$$\begin{aligned}\overline{u}^{01}&=a^{01}\mathrm{e}^{+\mathrm{i}kx^{01}}+d^{01}\mathrm{e}^{-\mathrm{i}kx^{01}}-p_1\mathrm{e}^{-\mathrm{i}k_1x^{01}},\\ \overline{u}^{10}&=a^{10}\mathrm{e}^{+\mathrm{i}kx^{10}}+d^{10}\mathrm{e}^{-\mathrm{i}kx^{10}}+p_1\mathrm{e}^{-\mathrm{i}k_1(l-x^{10})},\end{aligned} \tag{38}$$

where we have noticed the fact that in the 1-0 coordinate, the force moves from $x^{10}=l$ to $x^{10}=0$ with the positive direction of force also reversing. If the bar is fixed–fixed, we can obtain the scattering relation as

$$\left\{\begin{array}{c}d^{01}\\ d^{10}\end{array}\right\}=\left[\begin{array}{cc}-1 & 0\\ 0 & -1\end{array}\right]\left\{\begin{array}{c}a^{01}\\ a^{10}\end{array}\right\}+\left\{\begin{array}{c}p_1\\ -p_1\mathrm{e}^{-\mathrm{i}k_1l}\end{array}\right\}\quad\text{or}\quad\mathbf{d}=\mathbf{S}\mathbf{a}+\mathbf{q}_1. \tag{39}$$

For other boundary conditions, only the elements of the scattering matrix $\mathbf{S}$ change.

The displacements in the dual coordinates should be compatible to each other, i.e.

$$\overline{u}^{01}(x^{01},\omega)=-\overline{u}^{10}(l-x^{01},\omega) \tag{40}$$

from which we obtain

$$\left\{\begin{array}{c}a^{01}\\ a^{10}\end{array}\right\}=\left[\begin{array}{cc}-\mathrm{e}^{-\mathrm{i}kl} & 0\\ 0 & -\mathrm{e}^{-\mathrm{i}kl}\end{array}\right]\left\{\begin{array}{c}d^{10}\\ d^{01}\end{array}\right\}\quad\text{or}\quad\mathbf{a}=\mathbf{P}\mathbf{U}^0\mathbf{d}, \tag{41}$$

where $\mathbf{U}^0$ is the permutation matrix defined by Eq. (15). Combining Eq. (39) with Eq. (41) gives the final equation that is similar to Eq. (19). It is interesting to note that for the case of a point moving load, the source term comes from the scattering relation, differing from the case of a continuously distributed load.

4.2. A non-uniform bar subjected to a point moving load

If the bar is non-uniform, then the piece-wise uniform bar model shown in Fig. 1(b) shall be employed. Since the point load is moving along the whole non-uniform bar, at different moment, it will traverse different sub-bars. For the sub-bar acted by the point moving load, the governing equation in the frequency domain is shown in Eq. (36), while for the sub-bar in absence of the load, the governing equation is given by

$$\frac{\mathrm{d}^2\overline{u}(x,\omega)}{\mathrm{d}x^2}+k^2\overline{u}(x,\omega)=0. \tag{42}$$

However, the different form of equation at different time will introduce significant inconvenience in the calculation. We thus employ a unified treatment in the following. Assume that we divide the bar into N equal sub-bars with the length of each sub-bar being L/N. In this case, the time for the load traversing each sub-bar will be $t_s=L/(Na_0)$. Hence, for the jth sub-bar, the governing equation in the time-domain under the local coordinate x^{IJ} can be written as (with superscripts IJ omitted)

$$\frac{\partial^2u(x,t)}{\partial x^2}=\frac{1}{c^2}\frac{\partial^2u(x,t)}{\partial t^2}-\{H[t-(j-1)t_s]-H(t-jt_s)\}p_e\delta[x+(j-1)L/N-a_0t], \tag{43}$$

where $H(\cdot)$ is the Heaviside step function. Eq. (43) then can be transformed into the frequency domain as

$$\frac{\mathrm{d}^2\overline{u}(x,\omega)}{\mathrm{d}x^2}+k^2\overline{u}(x,\omega)=\overline{F}_1(x,\omega)+\overline{F}_2(x,\omega), \tag{44}$$

where $\overline{F}_1(x,\omega)=-(p_e/a_0)\mathrm{e}^{-\mathrm{i}\omega[x/a_0+(j-1)t_s]}$ and $\overline{F}_2(x,\omega)=(p_e/a_0)\mathrm{e}^{-\mathrm{i}\omega(jt_s)}\delta(x-L/N)$. Note that $\overline{F}_2(x,\omega)$ could be viewed as an external concentrated load applied at the right end, say joint J, of the sub-bar IJ. In this case, we could solve Eq. (44) only with $\overline{F}_1(x,\omega)$ and change the continuity conditions at joint J to

$$\overline{u}^{JI}+\overline{u}^{JK}=0,\quad \overline{f}^{JI}=\overline{f}^{JK}+\frac{p_e}{a_0}\mathrm{e}^{-\mathrm{i}\omega(jt_s)}\quad \text{at } x^{JI}=x^{JK}=0. \tag{45}$$

The solution of Eq. (44) with $\overline{F}_1(x,\omega)$ only is

$$\overline{u}(x,\omega)=a\mathrm{e}^{\mathrm{i}kx}+d\mathrm{e}^{-\mathrm{i}kx}-p_1\mathrm{e}^{-\mathrm{i}\omega[x/a_0+(j-1)t_s]}. \tag{46}$$

The following derivation is then similar and omitted here for brevity.

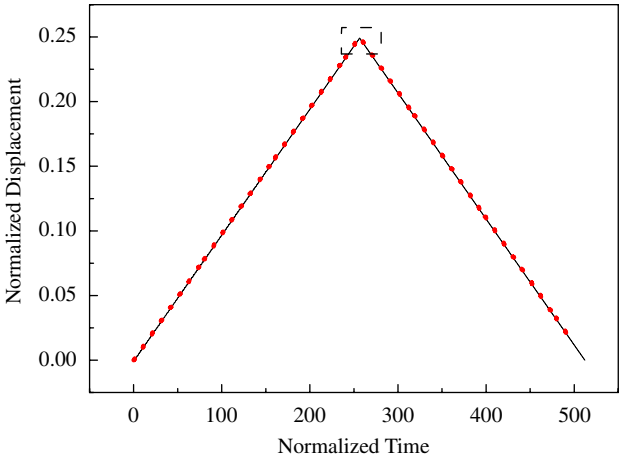

Fig. 9. Normalized displacement U at $\xi=0.5$. — MRRM. ····· MME.

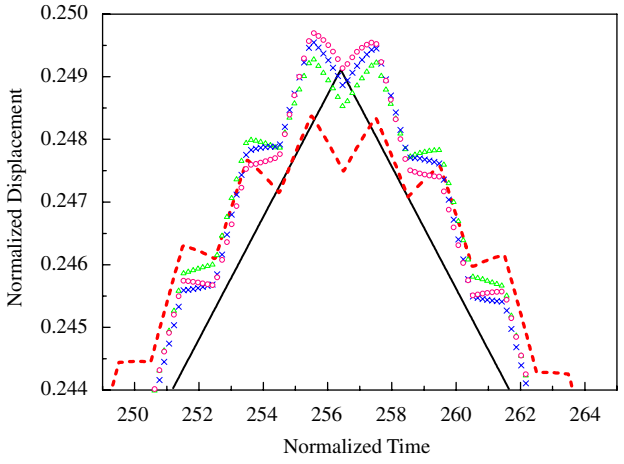

Fig. 10. Comparison of normalized displacement U at $\xi=0.5$. — MRRM. ····· MME ($n=50$). △ MME ($n=100$). × MME ($n=150$). ○ MME ($n=250$).

4.3. Numerical results

As a numerical example, consider a uniform rod with both ends fixed, subjected to a point moving load $p(x,t) = EA_0\delta(x - a_0t)$ with the speed $a_0 = 20\,\mathrm{m/s}$, and the length of the rod $L = 1\,\mathrm{m}$. The results are shown in Fig. 6, and are compared with those obtained by the method of mode expansion (MME) [10]. In the later method, the first 250 modes are used in the calculation. The two results are found to agree with each other very well. In particular, with the increasing number (n) of modes, MME predicts better and better results when compared with those obtained by MRRM, as shown in Figs. 9 and 10 clearly.

5. Conclusions

In this paper, the MRRM is extended to analyze the wave propagation in a bar subjected to continuously distributed loads and point moving loads. The particular solutions of the wave equations are obtained and the compatibility condition of displacements in dual local coordinates is employed to derive the phase relations. Different from the cases of concentrated external loads applied at the joints only, the source term appears in the phase relation for the distributed load. Several examples, either theoretical or numerical, are considered. Good agreement with existing results is obtained, validating the application of MRRM for different types of loadings and the correctness of the derived formulations. Regarding the method of equivalent nodal forces, the numerical example shows that, a certain large number of artificially divided elements are required to obtain an accurate dynamic response, especially for the axial force.

It is noted that the MRRM is based on continuum models, and hence there is no discretization error as usually encountered in the FEM, boundary element method or finite difference method. Compared with other continuum model-based methods, such as the spectral element method [9] and the method of transfer matrix (MTM) [13], MRRM is numerically stable and more accurate in obtaining transient responses of structures. A more detailed comparison of MRRM with MTM can be found in a recent review article by Pao et al. [7].

The present work makes a key step for the application of MRRM in a wider range of engineering problems. Although we consider only the bar model in this paper, the formulations for other types of structures could be deduced similarly. It is hoped that the method developed here could help analyzing the wave propagation in some structures where axial waves and flexural waves may couple at junctions through the joint conditions [1,2], and it is also especially hoped that the investigation would be useful to the NDT of engineering structures based on their dynamic behavior.

Acknowledgments

The work was supported by the National Natural Science Foundation of China (nos. 10472103, 10432030, and 10725210), the Specialized Research Fund for the Doctoral Program of Higher Education (no. 20060335107) and the Program for New Century Excellent Talents in University (no. NCET-05-05010). The authors are grateful to the anonymous reviewers for their constructive comments, which make improvement of our paper. Very special thanks are also extended to Professor Pao for his instruction and valuable suggestions.

References

[1] S.M. Howard, Y.H. Pao, Analysis and experiments on stress waves in planar trusses, *Journal of Engineering Mechanics* 124 (1998) 884–891.
[2] Y.H. Pao, D.C. Keh, Dynamic response and wave propagation in plane trusses and frames, *AIAA Journal* 37 (1999) 594–603.
[3] J.F. Chen, Y.H. Pao, Effects of causality and joint conditions on method of reverberation-ray matrix, *AIAA Journal* 41 (2003) 1138–1142.
[4] Y.H. Pao, X.Y. Su, J.Y. Tian, Reverberation matrix method for propagation of sound in a multilayered liquid, *Journal of Sound and Vibration* 230 (2000) 743–760.
[5] X.Y. Su, J.Y. Tian, Y.H. Pao, Application of the reverberation-ray matrix to the propagation of elastic waves in a layered solid, *International Journal of Solids and Structures* 39 (2002) 5447–5463.

[6] Y.H. Pao, G. Sun, Dynamic bending strains in planar trusses with pinned or rigid joints, *Journal of Engineering Mechanics* 129 (2003) 324–332.
[7] Y.H. Pao, W.Q. Chen, X.Y. Su, The reverberation-ray matrix and transfer matrix analyses of unidirectional wave motion, *Wave Motion* 44 (2007) 419–438.
[8] Q.S. Li, J.Q. Fang, A.P. Jeary, Free vibration analysis of cantilevered tall structures under various axial loads, *Engineering Structures* 22 (2000) 525–534.
[9] J.F. Doyle, *Wave Propagation in Structures: Spectral Analysis Using Fast Discrete Fourier Transforms*, Springer, New York, 1997.
[10] H. Matsuda, T. Sakiyama, C. Morita, M. Kawakami, Longitudinal impulsive response analysis of variable cross-section bars, *Journal of Sound and Vibration* 181 (3) (1995) 541–551.
[11] L. Frýba, *Vibration of Solids and Structures under Moving Loads*, Noordhoff, Groningen, 1972.
[12] I. Elishakoff, *Eigenvalues of Inhomogeneous Structures: Unusual Closed-Form Solutions*, CRC Press, Boca Raton, FL, 2005.
[13] E.C. Pestel, F.A. Leckie, *Matrix Methods in Elasto Mechanics*, McGraw-Hill, New York, 1963.